

On the Robustness of Deep Reinforcement Learning in IRS-Aided Wireless Communications Systems

Amal Feriani, Amine Mezghani, *Member, IEEE*, and Ekram Hossain, *Fellow, IEEE*

Abstract—We consider an Intelligent Reflecting Surface (IRS)-aided multiple-input single-output (MISO) system for downlink transmission. We compare the performance of Deep Reinforcement Learning (DRL) and conventional optimization methods in finding optimal phase shifts of the IRS elements to maximize the user signal-to-noise (SNR) ratio. Furthermore, we evaluate the robustness of these methods to channel impairments and changes in the system. We demonstrate numerically that DRL solutions show more robustness to noisy channels and user mobility.

Keywords: Intelligent Reflecting Surface (IRS), downlink transmission, optimal phase shift, Deep Reinforcement Learning (DRL), imperfect Channel State Information (CSI), Vector Approximate Message Passing (VAMP) algorithm, Alternating Direction Method of Multipliers (ADMM) algorithm

I. INTRODUCTION

Recently, Deep Reinforcement Learning (DRL) has attracted a lot of interest to solve a wide range of wireless communications problems [1], [2]. Thanks to its learning capabilities and inference speed, DRL has shown competitive performance compared to traditional optimization methods. This is why DRL-based algorithms are considered as one of the key technologies for future wireless generations. In the same vein, Intelligent Reflecting Surfaces (IRS) represent a promising pillar of the future wireless evolution since they are able to provide additional gain in wireless system performance at a low cost.

DRL has been already applied to solve IRS-related problems such as passive/active beamforming. In [3], the authors considered a Multiple-Input Single-Output (MISO) system and used DRL to find optimal passive phase shifts. The DRL agent achieves a better performance than the fixed-point iteration algorithm and results close to a SemiDefinite Relaxation (SDR) upper bound. The joint optimization of transmit beamforming and phase shifts in multi-user MISO network was proposed in [4] where the authors used a unified DRL algorithm to solve it. Furthermore, [5] approached the problem of minimization of the Base Station (BS) transmit power in MISO system using DRL for passive beamforming and traditional optimization-based method for active beamforming. An IRS-assisted downlink

NOMA multi-user system was studied in [6] and DRL was employed to predict the IRS phase shifters. DRL showcases better sum-rate performance compared to the OMA scheme. The objective of this paper is twofold: First, we provide a comparison between DRL methods and the best performing traditional optimization methods such as Vector Approximate Message Passing (VAMP) [7] and Alternating Direction Method of Multipliers (ADMM) [8] in solving the phase shift optimization problem for IRS-aided wireless communications systems. This work will help to build a benchmark to compare DRL to other exiting techniques. Furthermore, unlike the works mentioned above, our aim is not to solve passive beamforming with DRL but to motivate the use of DRL over other conventional methods in practical settings. For instance, we focus on the robustness of the optimal solution to channel impairments. To do so, we compare the decrease in the achieved SNR when the Channel State Information (CSI) is perturbed (i.e. additional noise) and the user location changes. Our work is novel since we consider that the agent's knowledge of the environment is not perfect and we test the obtained solution under different perturbation scenarios. Our objective through this work is to bring a more practical perspective to the proposed algorithms for phase shift optimization and to wireless problems in general. Simulation results show that, compared to other optimization methods, DRL is more robust to changes in the system. This is another advantage of DRL methods along with the inference speed that motivates the use of learning-based techniques to solve wireless problems.

The rest of the paper is organized as follows. The system model, assumptions, and the problem formulation are presented in Section II. The DRL-based approach for phase-shift optimization is presented in Section III. The performance evaluation and benchmarking results are presented in Section IV before the paper is concluded in Section V.

II. SYSTEM MODEL AND PROBLEM FORMULATION

Consider a BS equipped with N antenna elements serving a single-antenna user in the downlink. An IRS, with $M = M_x \times M_y$ reflective elements, is deployed to assist the BS. M_x and M_y refer to the number of IRS elements in each row and column, respectively. We denote by $\mathbf{H}_{bu} \in \mathbb{C}^{N \times 1}$, $\mathbf{H}_{ru} \in \mathbb{C}^{M \times 1}$, and $\mathbf{H}_{br} \in \mathbb{C}^{M \times N}$ the direct channel between the BS and the user, the channel between the IRS and the user and the MIMO channel linking the BS and the IRS (Fig. 1). Henceforth, the received signal at the user is

The authors are with the Department of Electrical and Computer Engineering at the University of Manitoba, Canada (emails: {feriania@myumanitoba.ca, Amine.Mezghani@umanitoba.ca, Ekram.Hossain@umanitoba.ca})

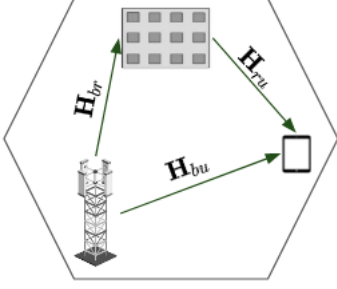


Fig. 1: IRS-aided single-user MISO system.

given by:

$$y = (\mathbf{H}_{bu}^H + \mathbf{H}_{ru}^H \Phi \mathbf{H}_{br}) \mathbf{F} s + n$$

where s is a zero-mean and unit-variance transmit symbol, $n \sim \mathcal{CN}(0, \sigma_n^2)$ is the additive white Gaussian noise. $\mathbf{F} \in \mathbb{C}^{N \times 1}$ is the beamforming vector satisfying the constraint $\|\mathbf{F}\|^2 = P_{max}$ with P_{max} being the BS maximum transmit power. $\Phi = \text{Diag}(\phi_1, \dots, \phi_M) \in \mathbb{C}^{M \times M}$ is the IRS phase shift matrix such that $\phi_i = e^{j\theta_i}$ with $\theta_i \in [0, 2\pi]$ representing the phase shift of the i th IRS reflective element for $i = 1, \dots, M$. Consequently, the user's effective channel is expressed as follows:

$$\mathbf{H}^H = \mathbf{H}_{bu}^H + \mathbf{H}_{ru}^H \Phi \mathbf{H}_{br}.$$

Furthermore, we assume that the channels are quasi-static frequency flat-fading and the CSI is available at the BS. The received SNR at the user is given by

$$\rho = \frac{|\mathbf{H}^H \mathbf{F}|^2}{\sigma_n^2}. \quad (1)$$

We seek to optimize the phase shift matrix Φ and the beamforming vector to maximize the user SNR. The optimization problem can be stated as follows:

$$\begin{aligned} \max_{\Phi, \mathbf{F}} \quad & \|(\mathbf{H}_{bu}^H + \mathbf{H}_{ru}^H \Phi \mathbf{H}_{br}) \mathbf{F}\|_2^2 \\ \text{s.t.} \quad & \|\mathbf{F}\|^2 = P_{max} \\ & |\Phi_{i,i}|^2 = 1. \end{aligned}$$

For this MISO system, we know that, for a fixed Φ , the optimal beamforming vector that maximizes the SNR is given by the maximum-ratio transmission (MRT) method [9] as follows:

$$\mathbf{F}^* = \frac{\sqrt{P_{max}} \mathbf{H}}{\|\mathbf{H}\|_2}. \quad (2)$$

Hence, the optimization problem can be simplified as:

$$(P_1) : \max_{\Phi} \quad \|\mathbf{H}_{bu}^H + \mathbf{H}_{ru}^H \Phi \mathbf{H}_{br}\|_2^2 \quad (3)$$

$$\text{s.t.} \quad |\Phi_{i,i}|^2 = 1, \quad i = 1, \dots, M. \quad (4)$$

The optimization problem as formulated in (P_1) is a non-convex problem due to the unimodular constraints.

Several works attempted to solve this optimization problem. In particular, [10] focused on minimizing the Minimum Mean Square Error (MMSE) criterion which is equivalent to maximizing the user SNR according to the I-MMSE relationship. The authors derived a closed-form solution for the beamforming vector and proposed a modified algorithm based on VAMP algorithm. This work shows better performance compared to ADMM and has a complexity of $O(NM + M^2 + N^3)$. The disadvantages of this method are two-fold: (i) it is an iterative algorithm, and (ii) it requires the perfect knowledge of CSI. In [11], the authors used an SDR method which is characterized by a high complexity (i.e. $O((M+1)^6)$).

To overcome the above-mentioned shortcomings of traditional optimization methods, DRL is used to learn the optimal phase shifts. The advantage of DRL compared to the previous methods is, it can be queried in real-time and necessitates less CPU time. A comparison between SDR and DRL-based solutions for (P_1) was presented in [3]. In this work, we provide a comparison between VAMP, ADMM, and DRL in addition to a performance analysis under different channel impairments.

III. DRL-BASED APPROACH

A. Background

The standard reinforcement learning framework consists of an agent learning to maximize its expected cumulative rewards through interacting with an environment. At each interaction or timestep t , given an observation s_t , the agent chooses an action a_t and receives an instantaneous reward r_t , and the system transit to a new state s_{t+1} . The tuples (s_t, a_t, r_t, s_{t+1}) constitute the agent experiences used for learning the optimal policy $\pi : S \mapsto \mathcal{P}(A)$. This learning problem is often modeled as a Markov Decision Process (MDP), described by the tuple (S, A, P, R, γ) , when the state space is fully-observable. S and A define the state and the action spaces, respectively; $P := S \times A \mapsto [0, 1]$ denotes the transition probability function, $R := S \times A \times S \mapsto R$ is the reward function, and $\gamma \in [0, 1]$ is a discount factor that trades-off the immediate and upcoming rewards.

We define the agent's expected return as the sum of the *discounted* future rewards $R_t = \mathbb{E} \left[\sum_{i=t}^T \gamma^{(i-t)} R(s_i, a_i, s_{i+1}) | a_i \sim \pi(\cdot | s_i) \right]$. Thus, the agent's objective is to maximize the expected long-term reward $J = \mathbb{E}_{\pi} \left[\sum_{t=0}^{\infty} \gamma^t R_t \right]$.

Another well-known function used to measure the agent's returns is the action-value function Q . It measures the expected accumulated rewards after executing an action a_t at a state s_t and following the policy π thereafter:

$$Q^{\pi}(s, a) = \mathbb{E} \left[\sum_{t=0}^{\infty} \gamma^t R(s_t, a_t, s_{t+1}) | a_t \sim \pi(\cdot | s_t), s_0 = s, a_0 = a \right].$$

The famous Q -learning algorithm makes use of the *Temporal Difference* (TD) formulation where the Q function is learned using the following recursive expression

$$Q(s_t, a_t) = (1 - \alpha)Q(s_t, a_t) + \alpha[r(s_t, a_t) + \gamma \max_{a'} Q(s_{t+1}, a')] \quad (5)$$

in which α is a learning rate.

The main disadvantage of the Q -learning method is the max operator in (5) which limits it to discrete action spaces. In this context, Deterministic Policy Gradient (DPG) algorithm [12] can be considered as an extension of Q -learning to continuous action spaces by replacing the $\max_{a'} Q(s_{t+1}, a')$ in (5) by $Q(s_{t+1}, \mu(s_{t+1}))$, where $\mu(s_{t+1}) = \arg \max_{a'} Q(s_{t+1}, a')$. Thus, DPG algorithms concurrently learn a Q -function Q_ϕ and a policy μ_ψ , where ϕ and ψ are the parameters of the Q -function and the policy, respectively. The Q -function is learned by minimizing the *Bellman error* in (6). As for the policy, the objective is to learn a *deterministic policy* that outputs the action corresponding to $\max_a Q_\phi(s, a)$. The policy is called deterministic because it gives the exact action to take at each state s . Hence, the learning process consists in performing gradient ascent with respect to θ to solve the objective in (8):

$$\phi^* = \arg \min_{\phi} \frac{1}{2} \sum_{(s, a, r, s')} \|Q_\phi(s, a) - y\|^2 \quad (6)$$

$$y = R(s, a) + \gamma \hat{Q}_{\phi'}(s', \hat{\mu}_{\psi'}(s')) \quad (7)$$

$$J(\theta) = \mathbb{E}_{s \sim D} \left[Q_\phi(s, \mu_\theta(s)) \right] \quad (8)$$

$$\nabla_{\theta} J(\theta) = \mathbb{E}_{s \sim D} \left[\nabla_{\theta} \mu_{\theta}(s) \nabla_a Q_{\phi}(s, a) \Big|_{a=\mu_{\theta}(s)} \right] \quad (9)$$

where \hat{Q} and $\hat{\mu}$ are called target networks which are copies of the Q and μ . These target networks are used to compute the target values [7]. The target parameters are updated using a Polyak update with a parameter τ .

Deep Deterministic Policy Gradient (DDPG) [13] has been widely used to solve wireless communication problems. It is an extension of the DPG method where the policy μ_ψ and the critic Q_ϕ are both deep neural networks.

B. MDP Formulation

The optimization problem in (P_1) is modeled as an MDP where the agent is the BS. In what follows, we define the state and action spaces and the reward function:

- **State space** S : consists of the user SNR and action $s_t = [\rho_{t-1}, a_{t-1}]$. The dimension of state space is $M + 1$ and spans \mathbb{R}_+ . Using the past actions helps mimicking the recurrent version of RL.
- **Action space** A : at each timestep, the agent chooses the phase shifts $\theta_i, i = 1 \dots M$. Thus, the dimension of the action space is M and $a_t = [\theta_1, \dots, \theta_M] \in [0, 2\pi]^M$.

- **Reward**: at each time step, the agent's reward is the received SNR as defined in (1).

Technically, this formulation can be considered as a partially observable MDP since the agent observes only its SNR and does not have access to the CSI which is used to compute the next state. So, the agent needs to infer the CSI in order to recover the full state. In this paper, we will solve this problem by using a model-free RL algorithm. In future works, other methods can be considered to deal with the problem of partial observability of the environment.

We assume that the agent interacts with the environment in an episodic manner. An episode ends when the number of time-steps exceeds a fixed horizon T . At the beginning of each episode, we sample new channel realizations and randomly choose the phase shifts to compute the first state s_0 .

The pseudo-code in **Algorithm 1** summarizes the DDPG algorithm to find the optimal phase shifts. To ensure a better exploration, we add an adaptive parameter space noise [14] in addition to the action space noise. The parameter noise is applied to the weights of the actor network. The traditional action noise makes the policy stochastic and enables the perturbation of action likelihoods independently from the state. However, the parameter space noise incorporates the noise directly in the parameters yielding a *state-dependent* exploration [15]. For more details, we refer the reader to [14].

IV. NUMERICAL RESULTS

A. Simulation Setup

In this section, we detail the experimental setup used to generate the results.

Channel models: The channel between the BS and the user is assumed to experience Rayleigh fading which suggests that the line-of-sight (LOS) signal between them is blocked:

$$\mathbf{H}_{bu} = \sqrt{G_{bu}} \mathbf{h}_{bu}$$

where $\mathbf{h}_{bu} \in \mathbb{C}^{N \times 1}$ and its elements are sampled independently from $\mathcal{CN}(0, 1)$. The channel between the BS and IRS as well as the one between the IRS and the user are Ricean fading:

$$\mathbf{H}_{br} = \sqrt{G_{br}} \left(\sqrt{\frac{K_1}{K_1 + 1}} \mathbf{H}_{br}^{LOS} + \sqrt{\frac{1}{K_1 + 1}} \mathbf{H}_{br}^{NLOS} \right)$$

$$\mathbf{H}_{ru} = \sqrt{G_{ru}} \left(\sqrt{\frac{K_2}{K_2 + 1}} \mathbf{H}_{ru}^{LOS} + \sqrt{\frac{1}{K_2 + 1}} \mathbf{H}_{ru}^{NLOS} \right)$$

where \mathbf{H}_{br}^{LOS} and \mathbf{H}_{ru}^{LOS} are the deterministic LOS components for IRS-user and BS-IRS links computed as shown [3]. \mathbf{H}_{br}^{NLOS} and \mathbf{H}_{ru}^{NLOS} are the NLOS components independently distributed as $\mathcal{CN}(0, 1)$. K_1 and K_2 represent the Ricean factors.

The path-loss model is given by $G(d) = G_0 - 10\alpha \log_{10}(d/d_0)$ in dB, where G_0 is the path-loss at the

Algorithm 1 DDPG with Parameter Noise Exploration

- 1: **Input:** Initialize actor parameters ψ , critic parameters ϕ , empty memory buffer \mathcal{D} , parameter space noise standard deviation σ_0 , intervals for training and noise adaptive scaling, T_{train} , T_{adapt} , number of training steps N_{train} , an adaption update coefficient α and threshold δ
 - 2: Initialize the target networks parameters $\phi' \leftarrow \phi$ and $\psi' \leftarrow \psi$
 - 3: Set $\tilde{\mu} = \mu_{\tilde{\psi}}$ for exploration and $\bar{\mu} = \mu_{\tilde{\psi}}$ for noise adaption, $t = 0$
 - 4: **repeat**
 - 5: Apply noise perturbation to actor parameters $\tilde{\psi} \leftarrow \psi + \mathcal{N}(0, \sigma_k^2 \mathbf{I})$ to obtain $\tilde{\mu}$
 - 6: Receive state \mathbf{s}_t and choose an action $\mathbf{a}_t = \text{clip}(\tilde{\mu}(\mathbf{s}_t) + \epsilon, A_{\text{low}}, A_{\text{high}})$ according to the perturbed policy $\tilde{\mu}$ where $\epsilon \sim \mathcal{N}(0, \sigma_a)$
 - 7: Execute \mathbf{a}_t and observe the receive reward r , the next state \mathbf{s}^{t+1} . Store $(\mathbf{s}_t, \mathbf{a}_t, r, \mathbf{s}_{t+1})$ in \mathcal{D}
 - 8: If \mathbf{s}^{t+1} is terminal, reset the environment and update the perturbed actor $\tilde{\psi} \leftarrow \psi + \mathcal{N}(0, \sigma_k^2 \mathbf{I})$
 - 9: $t = t + 1$
 - 10: **if** $t \bmod T_{\text{train}}$ **then**
 - 11: **for** $i = 0, \dots, N_{\text{train}}$ **do**
 - 12: Sample a minibatch \mathcal{B} from \mathcal{D}
 - 13: Update the actor and the critic parameters as specified by (6), (9)
 - 14: Update target networks
 - 15: $\phi' \leftarrow \tau \phi + (1 - \tau) \phi'$
 - 16: $\psi' \leftarrow \tau \psi + (1 - \tau) \psi'$
 - 17: **if** $i \bmod T_{\text{adapt}}$ **then**
 - 18: Perturb $\tilde{\psi} \leftarrow \psi + \mathcal{N}(0, \sigma_k^2 \mathbf{I})$ and obtain $\bar{\mu}$
 - 19: Estimate the standard deviation between μ and $\bar{\mu}$
 - 20: $d_k = \mathbb{E}_{\mathbf{s}} \left[\sqrt{\frac{1}{|\mathcal{A}|} \sum_{j=1}^{|\mathcal{A}|} (\mu(\mathbf{s})_j - \bar{\mu}(\mathbf{s})_j)^2} \right]$
 - 21: Adapt the parameter noise scale
 - 22: $\sigma_{k+1} \leftarrow \begin{cases} \alpha \sigma_k & \text{if } d_k \leq \delta, \\ \frac{1}{\alpha} \sigma_k & \text{otherwise} \end{cases}$
 - 23: **end if**
 - 24: **end for**
 - 25: **end if**
 - 26: **until** convergence
-

reference distance, d_0 is the reference distance and α is the path loss exponent.

Simulation hyperparameters: Table I summarizes the simulation parameters. For the DDPG algorithm, we use the hyperparameters reported in [3] in addition to the parameter space noise. We find that using a long episode horizon (i.e. 1000) is critical for learning.

Policy representation: For both actor and critic, the same architecture is used: a feedforward deep neural network with two hidden layers with 300 and 200 hidden units and Relu activations. Before applying the activation function, we use a normalization layer [16] to stabilize the learning under parameter noise.

Baselines: We compare the DRL agent with VAMP and ADMM algorithms due to their convergence guarantees and speed.

For reproducibility purposes, we will release the code of the environment used for the simulations below. [17] is used as an implementation of the DRL algorithm.

TABLE I: Simulation parameters

Parameter	Value
$K_1 = K_2$	10
N	10
M	50
σ_n^2	-80 dBm
P_{max}	5 dBm
d_0	1 m
G_0	-30 dB
$\alpha_{br}, \alpha_{bu}, \alpha_{ru}$	2, 2, 2.8
d_{br}, d_{bu}, d_{ru}	51, 48, 1.5 m
Hidden layers	300, 200
learning rate	$1e^{-3}$
Episode horizon H	1000
Replay buffer size	$1e^6$
$N_{\text{train}} = T_{\text{adapt}}$	50
T_{train}	1000
$\sigma_a = \sigma_0$	0.1

B. Results and Discussion

Performance comparison: We first compare the three considered methods: VAMP, ADMM, and DRL. Here, we set the parameters of the network as reported in Table I and vary the number of IRS elements. In Fig. 2, we illustrate the achievable SNR as a function of the number of IRS reflective elements for the different considered algorithms. The achievable SNR increases as the number of IRS elements increases. With perfect CSI, VAMP has the best achieved SNR compared to the other methods. We observe that the DRL method is able to achieve good performance compared to ADMM even without access to channel information. Fig. 3 shows that the agent's reward improves as the number of IRS elements increases. However, the SNR gain becomes smaller as the number of IRS elements gets higher.

Furthermore, we examine the inference speed of each algorithm and summarize them in Table II. We average the inference time over 1000 realizations. VAMP and ADMM algorithms are run for 30 iterations to achieve convergence [10]. After training, the DRL agent is queried in real-time to get the optimal phase shifts. Compared to traditional optimization techniques, DRL is superior in terms of inference speed which makes it more appealing for practical implementations.

TABLE II: Inference time in ms

M	VAMP	ADMM	DRL
50	30	19	0.3
100	38	29	0.48
144	48	41	0.49
196	76	64	0.6
256	100	100	0.62

Performance under unreliable channel: Since in real-world scenarios, the CSI acquired by the transmitter is not perfect and subject to errors, in this section we investigate the impact of CSI errors on the performance of the considered algorithms. As the first step, we obtain the optimal phase shifts and beamforming vector using the available CSI. Afterwards, we apply perturbations to the channels as

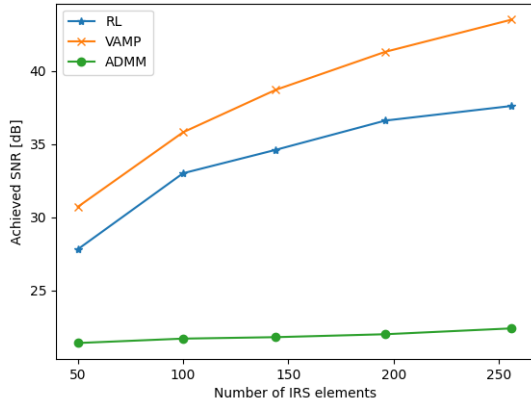


Fig. 2: Achieved SNR.

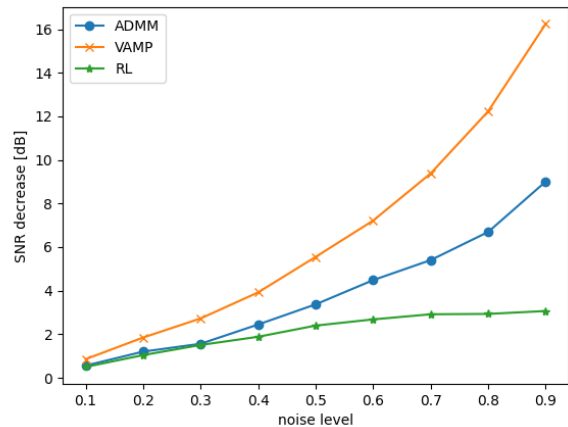


Fig. 4: The loss in SNR due to channel errors.

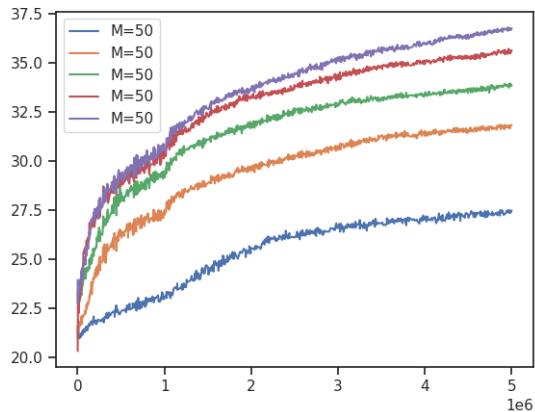


Fig. 3: DRL training curves for different number of IRS elements, shown in (10):

$$\mathbf{H}[t] = \sqrt{\epsilon}\mathbf{H}[t-1] + \sqrt{\epsilon-1}\mathbf{w}[t] \quad (10)$$

where $\mathbf{w}[t]$ contains independent and identically distributed $\mathcal{CN}(0, 1)$ elements. We compute the user SNR using the optimal phase shifts and the perturbed channels. Note that the objective is to study the impact of the channel errors on the optimal solutions. This means that we verify if the obtained solutions remain optimal with small changes in the CSI.

Fig. 4 illustrates the decrease in the user SNR due to different levels of noise. Since VAMP and ADMM rely on perfect CSI to find optimal solutions, the drop in performance is severe compared to DRL. Indeed, the DRL agent is able to learn a good policy without relying on the CSI directly which makes it more robust to changes in the environment. Furthermore, we observe that VAMP is more sensitive to changes in the channel than ADMM. For a high level of noise, VAMP performance drops by more than 16 dB whereas the performance of the DRL agent decreases only by 3 dB.

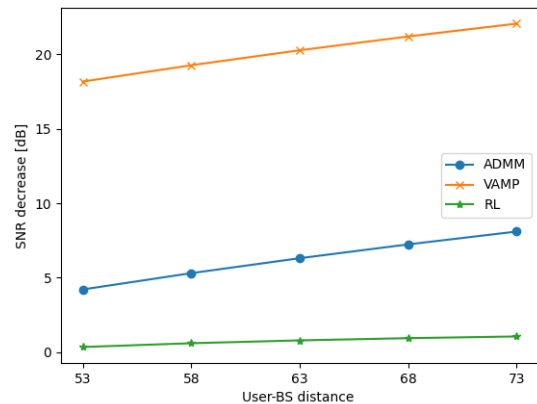


Fig. 5: The loss in SNR due to user mobility.

Performance under user mobility: To further verify the robustness of the DRL to changes in its environment, we increase the distance between the BS and the user to simulate a mobile target. Originally, the distance between the user and BS is 48 m. We assume that the user is moving away from the BS which represents the worst-case scenario. Hence, the distance is increased by a step-size in $[5, 25]$ m. Note that we first compute the optimal phase shifts and beamforming vector using the current CSI, then we increase the user distance and compute the SNR using the optimal solutions. A similar pattern is observed in Fig. 5 where VAMP and ADMM suffer dramatic drops in the user SNR. Surprisingly, the DRL performance stays approximately the same.

V. CONCLUSION

In this paper, we aimed to investigate the robustness of DRL against changes in CSI. This is a practical scenario where the CSI at the transmitter is subject to errors and noise. DRL shows an interesting resilience to different

channel impairments. This is advantageous compared to other optimization/inference methods where perfect CSI is crucial to ensure good performance. Furthermore, we provide a rigorous comparison between DRL, VAMP, and ADMM to optimize the phase shift matrix for downlink MISO transmission. Numerical results show that DRL is better than ADMM which fails to find a good solution for the considered system. Although VAMP has better performance, the DRL agent is capable of learning good policies without relying on any CSI.

In this work, we have only considered errors in the CSI; however, other sources of perturbations can impact the performance of the DRL agent. In a future work, we will do a more detailed investigation of the DRL methods for wireless continuous control. Furthermore, only robustness during inference is considered in this paper. Training under uncertainty can also be studied as an extension.

REFERENCES

- [1] Y. Al-Eryani, M. Akrouf, and E. Hossain, "Multiple access in cell-free networks: Outage performance, dynamic clustering, and deep reinforcement learning-based design," *IEEE Journal on Selected Areas in Communications*, vol. 39, no. 4, pp. 1028–1042, 2021.
- [2] Y. Al-Eryani, M. Akrouf, and E. Hossain, "Antenna clustering for simultaneous wireless information and power transfer in a mimo full-duplex system: A deep reinforcement learning-based design," *IEEE Transactions on Communications*, vol. 69, no. 4, pp. 2331–2345, 2021.
- [3] K. Feng, Q. Wang, X. Li, and C.-K. Wen, "Deep reinforcement learning based intelligent reflecting surface optimization for miso communication systems," *IEEE Wireless Communications Letters*, vol. 9, no. 5, pp. 745–749, 2020.
- [4] C. Huang, R. Mo, and C. Yuen, "Reconfigurable intelligent surface assisted multiuser miso systems exploiting deep reinforcement learning," *IEEE Journal on Selected Areas in Communications*, vol. 38, no. 8, pp. 1839–1850, 2020.
- [5] J. Lin, Y. Zou, X. Dong, S. Gong, D. T. Hoang, and D. Niyato, "Optimization-driven deep reinforcement learning for robust beamforming in irs-assisted wireless communications," *arXiv preprint arXiv:2005.11885*, 2020.
- [6] M. Shehab, B. S. Ciftler, T. Khattab, M. Abdallah, and D. Trincherro, "Deep reinforcement learning powered irs-assisted downlink noma," *arXiv preprint arXiv:2104.01414*, 2021.
- [7] S. Rangan, P. Schniter, and A. K. Fletcher, "Vector approximate message passing," *IEEE Transactions on Information Theory*, vol. 65, no. 10, pp. 6664–6684, 2019.
- [8] S. Boyd, N. Parikh, and E. Chu, *Distributed optimization and statistical learning via the alternating direction method of multipliers*. Now Publishers Inc, 2011.
- [9] Q. Wu and R. Zhang, "Beamforming optimization for intelligent reflecting surface with discrete phase shifts," in *ICASSP 2019-2019 IEEE International Conference on Acoustics, Speech and Signal Processing (ICASSP)*, pp. 7830–7833, IEEE, 2019.
- [10] H. U. Rehman, F. Bellili, A. Mezghani, *et al.*, "Joint active and passive beamforming for irs-assisted multi-user mimo systems: A vamp approach," *arXiv preprint arXiv:2102.01232*, 2021.
- [11] X. Yu, D. Xu, and R. Schober, "Miso wireless communication systems via intelligent reflecting surfaces," in *2019 IEEE/CIC International Conference on Communications in China (ICCC)*, pp. 735–740, IEEE, 2019.
- [12] D. Silver, G. Lever, N. Heess, T. Degris, D. Wierstra, and M. Riedmiller, "Deterministic policy gradient algorithms," in *Proceedings of the 31st International Conference on International Conference on Machine Learning*, pp. 387–395, 2014.
- [13] T. P. Lillicrap, J. J. Hunt, A. Pritzel, N. Heess, T. Erez, Y. Tassa, D. Silver, and D. Wierstra, "Continuous control with deep reinforcement learning," *arXiv preprint arXiv:1509.02971*, 2015.
- [14] M. Plappert, R. Houthoofd, P. Dhariwal, S. Sidor, R. Y. Chen, X. Chen, T. Asfour, P. Abbeel, and M. Andrychowicz, "Parameter space noise for exploration," *arXiv preprint arXiv:1706.01905*, 2017.
- [15] T. Rückstieß, M. Felder, and J. Schmidhuber, "State-dependent exploration for policy gradient methods," in *Joint European Conference on Machine Learning and Knowledge Discovery in Databases*, pp. 234–249, Springer, 2008.
- [16] J. L. Ba, J. R. Kiros, and G. E. Hinton, "Layer normalization," *arXiv preprint arXiv:1607.06450*, 2016.
- [17] A. Hill, A. Raffin, M. Ernestus, A. Gleave, A. Kanervisto, R. Traore, P. Dhariwal, C. Hesse, O. Klimov, A. Nichol, M. Plappert, A. Radford, J. Schulman, S. Sidor, and Y. Wu, "Stable baselines." <https://github.com/hill-a/stable-baselines>, 2018.